PAPER

CrossMark
click for updates

Halogen and hydrogen bonds in compressed pentachloroethane†

Maciej Bujak,*[a] Marcin Podsiadło[b] and Andrzej Katrusiak*[b]

In pentachloroethane, C_2HCl_5, high pressure initially strongly compresses the C–H···Cl bonds in phase I; however, in phase II which is stable above 0.62 GPa the role of hydrogen bonds is diminished and molecular aggregation is dominated by halogen bonds Cl···Cl. Both phases have been determined by X-ray diffraction and the phase diagram of C_2HCl_5 has been outlined. The transition between phases I and II retains some relation between their structures and reduces the symmetry from class *mmm* (space group *Pnma*) to $2/m$ (space group $P2_1/n11$). The discontinuous transition, with the shear strain exceeding 21°, is so strong that its progress can be visually observed even for powdered samples. The single-crystal growth suggests a surface-roughening transition, as phase I grows in the form of dendrites combining into oval plates, while phase II forms prisms with sharp edges.

Introduction

Ethane belongs to the simplest alkanes, present as building blocks in many organic molecules. Therefore, ethane and its derivatives are valuable model compounds for studying molecular aggregation and conformations. The application of halogenated alkanes for improving the technological properties of fuels used for airplanes and improving their security requires information about the structure, aggregation, interactions and thermodynamic properties of these compounds.[1] Halo-substituted methanes exhibit a variety of aggregation modes involving CH···halogen and halogen···halogen interactions.[2] Haloethanes additionally can change their conformation due to the relatively soft rotations about the C–C bond. Furthermore, the molecules can be orientationally and conformationally disordered.[3] Consequently, haloethanes exist in polymorphic forms and undergo phase transitions involving order–disorder, conformational conversions and changing types of intermolecular interactions.[3b,4] Presently, we have studied the aggregation of pentachloroethane, C_2HCl_5 (PCE). Its *staggered* conformation is strongly favored, and the Cl···Cl contacts are most likely to dominate its intermolecular interactions. We were particularly interested in the role of CH···Cl contacts, which are considerably shorter than halogen bonds Cl···Cl and for this reason could be excluded from the main cohesion forces.[5] We have applied high pressure for these studies, because it is the most efficient method for modifying the molecular structure and arrangement in crystals. Therefore, high pressure is increasingly often used for generating new polymorphs of pharmaceutical, energetic and other materials.[6]

Results and discussion

When isothermally compressed in a diamond-anvil cell (DAC), the liquid PCE sample first freezes in orthorhombic phase I and then transforms into monoclinic phase II (see Fig. 1 and Movie S1, ESI†). We determined its structure at 295 K/0.36 GPa and 295 K/0.45 GPa (Table 1). Still higher pressure of *ca.* 295 K/0.62 GPa induces a reversible discontinuous transition to monoclinic phase II (PCE-II, Fig. 2 and S1, ESI†). We determined the high-pressure structures of PCE-II,

[a] Faculty of Chemistry, University of Opole, Oleska 48, 45-052 Opole, Poland. E-mail: mbujak@uni.opole.pl; Tel: +48 (77) 452 7159

[b] Faculty of Chemistry, Adam Mickiewicz University, Umultowska 89b, 61-614 Poznań, Poland. E-mail: katran@amu.edu.pl; Tel: +48 (61) 829 1590
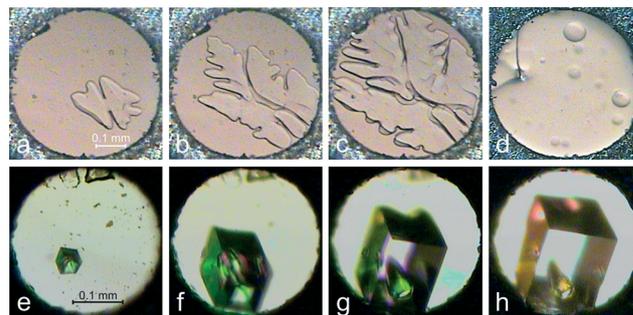
Fig. 1 Stages of isochoric growth of the PCE-I single crystal initially in the 'snowflake' dendritic, rounded nucleus grown from neat liquid at *ca.* 350 K and eventually fully filling the DAC chamber at 295 K/0.36 GPa (a–d), and the sample with well-defined faces of PCE-II grown from the PCE : propan-2-ol 1 : 1 (vol.) mixture at 0.76 GPa (e–h). Ruby chips for pressure calibration lie at the upper edge of the chambers.

Table 1 Selected crystal data of PCE phases I and II at 295 K. Note the exchanged axes [x] and [y] between phases I and II

	PCE-I		PCE-II	
Pressure, GPa	0.36(2)	0.45(2)	0.76(2)	1.00(2)
Crystal system	Orthorhombic	Orthorhombic	Monoclinic	Monoclinic
Space group	$Pnma$	$Pnma$	$P2_1/n$	$P2_1/n$
a, Å	10.325(8)	10.210(7)	9.5190(17)	9.4194(9)
b, Å	11.063(3)	11.039(3)	11.3199(4)	11.2200(3)
c, Å	6.0870(10)	6.0415(9)	6.393(3)	6.379(4)
β, °	90	90	111.78(3)	111.75(3)
V, Å^3	695.3(6)	680.9(5)	639.7(3)	626.2(4)
Z, Z'	4, 0.5	4, 0.5	4, 1	4, 1
ρ, g cm^{-3}	1.932	1.973	2.100	2.146
R_1 ($I > 2\sigma_I$)	0.1066	0.0997	0.0409	0.0282
R_1 (all data)	0.1260	0.1147	0.0501	0.0305
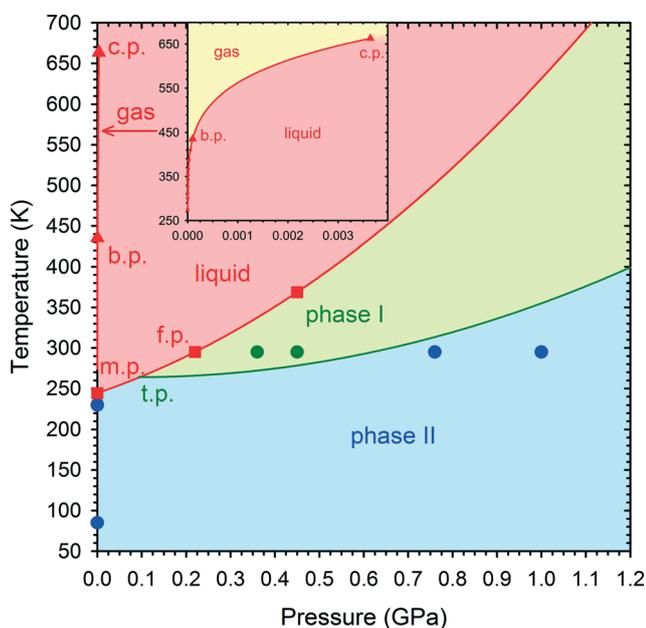
Fig. 2 The phase diagram of PCE based on visual observation of the liquid freezing in the diamond-anvil cell (red squares), X-ray diffraction data (green and blue circles) and literature information (*cf.* Fig. S1, ESI†). Triple point (t.p.) is deduced from the absence of transition between phases I and II at 0.1 MPa (see the DSC plot in Fig. S2, ESI†).

crystallized from the 1 : 1 (v/v) mixture of PCE and propan-2-ol, at 295 K/0.76 GPa and 295 K/1.00 GPa.

The comparison of unit-cell dimensions, positions of molecules in the unit cells (Fig. 3) and crystal symmetry group–subgroup relations indicate that phases I and II are structurally related. The transition reduces the symmetry of space-group $Pnma$ by eliminating the mirror plane and glide plane a. In order to comply with the convention, axes [x] and [y] of phase II have been exchanged and angle β becomes monoclinic in space group $P12_1/n1$ (Table 1). The lattice relation between phases I and II implies that parameter a_I corresponds to b_{II} and b_I corresponds to a_{II} (Fig. 4, the subscripts

indicate the phases). It also shows that the transition induces a huge strain between phases I and II: axis [x] of phase I expands by over 10%, axis [y] shrinks by nearly −15%, axis [z] expands by about 6% and a huge shear strain exceeds 21°. All these changes mutually compensate and the resultant volume drop is relatively small.

In both phases I and II, the PCE molecules retain the *staggered* conformation. In phase I, the molecules are located on mirror planes. Each molecule is involved in two Cl⋯Cl contacts and two CH⋯Cl bonds; the H⋯Cl distance becomes shorter than the sum of van der Waals radii above 0.45 GPa (ref. 7) (Table 2, Fig. 3a).

The pattern of halogen bonds changes between phases I and II (Fig. 3). In phase I at 295 K/0.45 GPa, the Cl⋯Cl bonds arrange molecules into *zigzag* chains along axis [y] and the voids also assume a *zigzag* motif of the same direction and period, but much larger amplitude (Fig. 3a). In phase II, the Cl⋯Cl contacts are more numerous and they form a 3-dimensional pattern (Fig. 3b).

The compression of PCE at room temperature (Fig. 4 and S3, ESI†) changes abruptly its volume by −1.3% when the liquid freezes at 0.22 GPa. This molecular-volume drop by 2.4 Å^3 is *ca.* twice smaller than that in 1112TCE (*ca.* 3.8 Å^3, −2.5%)^{4a} and it is the smallest volume change reported for chloroethanes,[3b,4a–c] which also corresponds to the smallest reduction of averaged intermolecular distances for PCE in the pressure region immediately before and above freezing. Then the compression of phase II, between 0.62 and 1.9 GPa, is on average almost three times smaller than that of phase I between 0.22 and 0.62 GPa. The volume discontinuity is very small, but different compression rates clearly distinguish the regions of phases I and II.

In phases I and II, the intermolecular Cl⋯Cl contacts have been compressed to 3.37 and 3.28 Å, respectively. Contacts H⋯Cl are the strongest compressed contacts in phase I, much stronger than contacts Cl⋯Cl. According to the CH⋯Cl bond compression within phase I, it can be estimated that the H⋯Cl distance is less than 2.8 or even 2.7 Å before the transition to phase II. In phase II, the H⋯Cl distance is longer than 3.0 Å and it increases with pressure (Fig. 5). It may indicate that high pressure reduces the potential energy (E_p) associated with the CH⋯Cl bonds in phase I. In phase II, two H⋯Cl contacts, somewhat longer than those in phase I, become longer as pressure increases. At the same time, the compression of contacts Cl⋯Cl in phase II is weaker than that in phase I. It thus appears that the structural rearrangement between phases I and II reverses the compression rate of contacts Cl⋯Cl and H⋯Cl (Tables 2 and 3; Fig. 5 and S4, ESI†). A relatively long, but commensurate with the sum of the van der Waals radii[7] H⋯Cl/CH⋯Cl intermolecular hydrogen bond was found only in the structure of PCE-I determined at 295 K/0.45 GPa.

The Hirshfeld two-dimensional fingerprint plots show that the H⋯Cl contacts are the most different feature of PCE-I and II (Fig. S5, ESI†), while in both polymorphs the dominant role is played by Cl⋯Cl contacts (Tables 2 and 3). It is
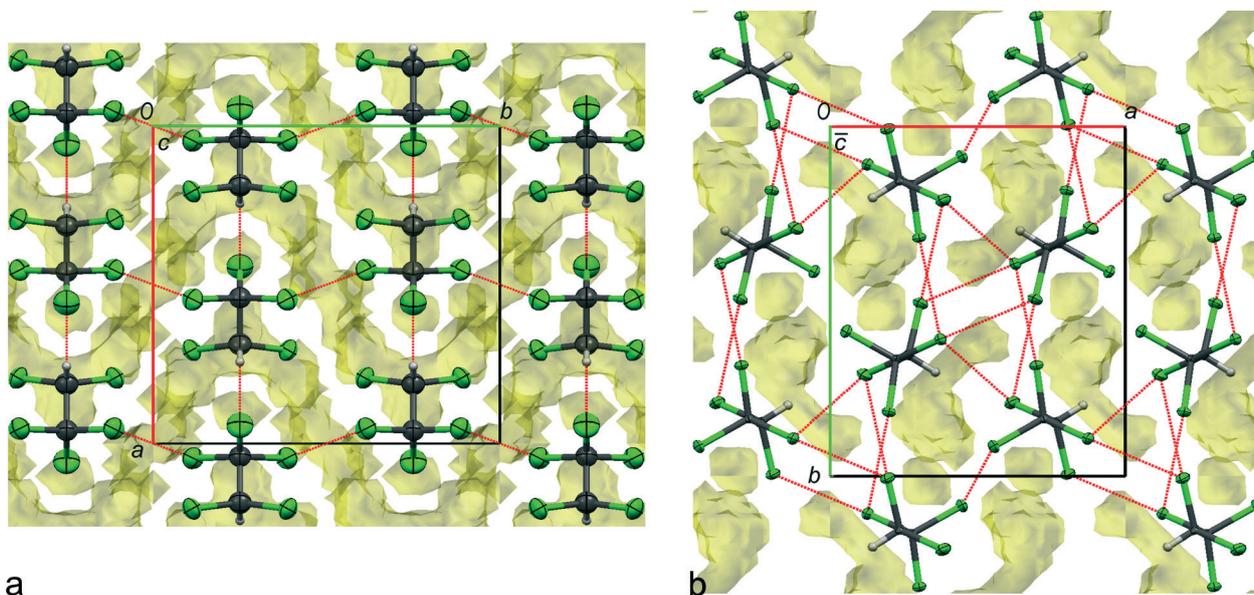
Fig. 3 The structures of PCE phase I at 295 K/0.45 GPa (a) and phase II at 295 K/1.00 GPa (b). The intermolecular space accessible to a probing sphere of radius 0.45 Å is indicated in yellow. This void volume is 13.8% in phase I and 7.8% in phase II. The dotted red lines indicate the shortest intermolecular Cl···Cl and H···Cl contacts. Displacement ellipsoids are plotted at the 15% probability level.
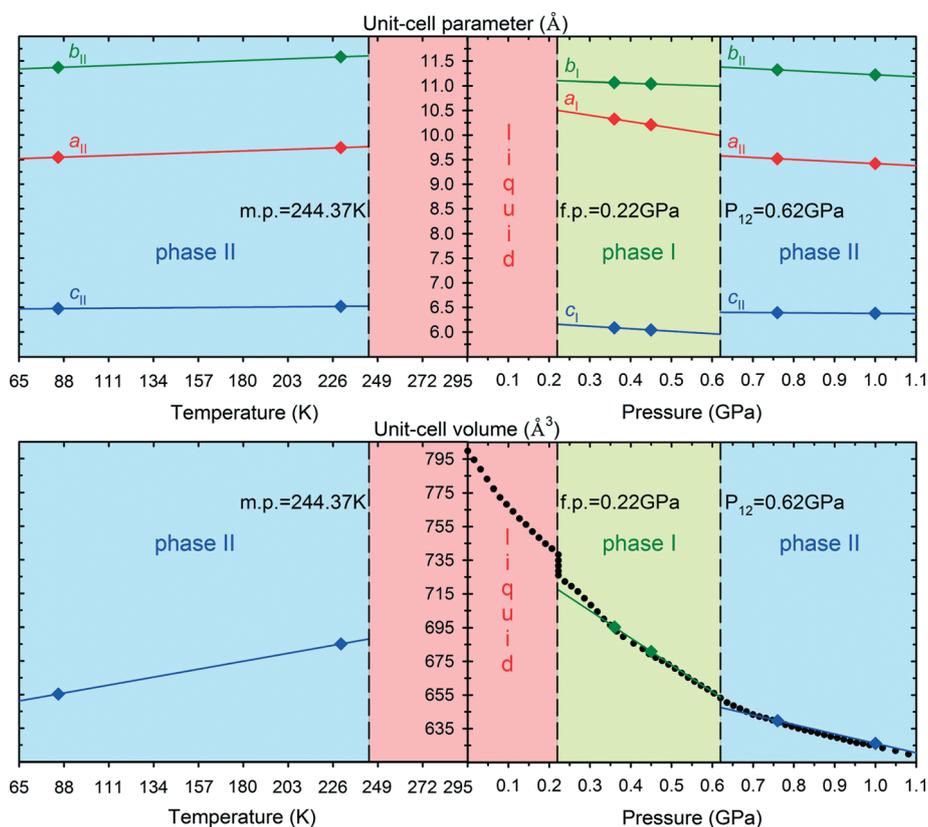

Fig. 4 Temperature and pressure dependence of unit-cell parameters a, b, c and unit-cell volume of PCE. The changes in monoclinic angle β are plotted in Fig. S6, ESI.†

remarkable that in phase I, the C–H···Cl bonds are formed, and the Cl···Cl contacts do not strictly conform to neither type I nor type II.[8]

The Cl···Cl contacts in phase II can be classified as halogen bonds of types I (Cl2···Cl2^V) and II (Cl1···Cl3^I) or somewhat distorted from these types (Table 3). The weaker

Table 2 Dimensions (Å, °) of the shortest intermolecular contacts in PCE-I at 295 K/0.36 GPa and 295 K/0.45 GPa

Temperature, K	295(2)	295(2)
Pressure, GPa	0.36(2)	0.45(2)
$Cl1 \cdots Cl1^{I}$	3.438(11)	3.373(10)
$C1-Cl1 \cdots Cl1^{I}$	160(2)	162(2)
$Cl1 \cdots Cl1^{I}-C1^{I}$	160(2)	162(2)
$C1-Cl1 \cdots Cl1^{I}-C1^{I}$	180.00(1)	180.00(1)
$H1 \cdots Cl2^{II}$	3.19	2.95
$C2-H1 \cdots Cl2^{II}$	175	172
$H1 \cdots Cl2^{II}-C1^{II}$	79	81
$C2-H1 \cdots Cl2^{II}-C1^{II}$	0.00	0.00
$C2 \cdots Cl2^{II}$	4.17(7)	3.92(6)
$C1-C2 \cdots Cl2^{II}$	110(3)	118(3)
$C2 \cdots Cl2^{II}-C1^{II}$	78(2)	79(2)
$C1-C2 \cdots Cl2^{II}-C1^{II}$	180.00	180.00

Symmetry codes: (I) $-x$, $1 - y$, $-1 - z$; (II) $1/2 + x$, y, $-1/2 - z$.

Table 3 Dimensions (Å, °) of the shortest intermolecular contacts in PCE-II at 295 K/0.76 GPa, 295 K/1.00 GPa, 230 K/0.1 MPa and 85 K/0.1 MPa

Temperature, K	295(2)	295(2)	230.0(1)	85.0(5)
Pressure	0.76(2) GPa	1.00(2) GPa	0.1 MPa	0.1 MPa
$Cl1 \cdots Cl3^{I}$	3.415(2)	3.3649(15)	3.5459(12)	3.4407(6)
$C1-Cl1 \cdots Cl3^{I}$	174.4(6)	175.7(4)	175.02(12)	175.71(6)
$Cl1 \cdots Cl3^{I}-C1^{I}$	106.8(2)	107.77(18)	107.56(11)	108.08(6)
$C1-Cl1 \cdots Cl3^{I}-C1^{I}$	169(3)	179(7)	170(1)	164.1(7)
$Cl3 \cdots Cl4^{II}$	3.332(6)	3.281(3)	3.4573(12)	3.3712(6)
$C1-Cl3 \cdots Cl4^{II}$	121.4(3)	119.6(2)	121.82(11)	121.19(6)
$Cl3 \cdots Cl4^{II}-C2^{II}$	161.1(4)	161.9(3)	164.36(12)	162.60(6)
$C1-Cl3 \cdots Cl4^{II}-C2^{II}$	$-168(1)$	$-170(2)$	$-172.6(5)$	$-165.6(2)$
$Cl3 \cdots Cl5^{III}$	3.438(6)	3.393(2)	3.5698(12)	3.4563(6)
$C1-Cl3 \cdots Cl5^{III}$	170.2(5)	171.6(6)	170.44(12)	169.85(6)
$Cl3 \cdots Cl5^{III}-C2^{III}$	113.1(7)	115.5(4)	115.37(13)	115.25(6)
$C1-Cl3 \cdots Cl5^{III}-C2^{III}$	60(1)	70(1)	61.2(7)	63.6(3)
$Cl4 \cdots Cl5^{IV}$	3.432(2)	3.3914(14)	3.5457(13)	3.4398(6)
$C2-Cl4 \cdots Cl5^{IV}$	101.4(3)	101.7(2)	103.77(12)	103.18(6)
$Cl4 \cdots Cl5^{IV}-C2^{IV}$	164.7(8)	166.8(6)	168.01(12)	166.24(6)
$C2-Cl4 \cdots Cl5^{IV}-C2^{IV}$	$-129(1)$	$-123(1)$	$-124.8(6)$	$-121.1(2)$
$Cl2 \cdots Cl2^{V}$	3.440(7)	3.414(6)	3.5763(18)	3.5438(9)
$C1-Cl2 \cdots Cl2^{V}$	132.9(7)	130.8(6)	134.48(12)	132.29(6)
$Cl2 \cdots Cl2^{V}-C1^{V}$	132.9(7)	130.8(6)	134.48(13)	132.29(6)
$C1-Cl2 \cdots Cl2^{V}-C1^{V}$	180.00	180.00	180.00	180.00

Symmetry codes: (I) $1/2 - x$, $1/2 + y$, $1/2 - z$; (II) $-1/2 + x$, $1/2 - y$, $1/2 + z$; (III) $-x$, $-y$, $-z$; (IV) $1/2 - x$, $1/2 + y$, $-1/2 - z$; (V) $1 - x$, $-y$, $1 - z$.

compression of the Cl⋯Cl contacts in phase II and even the negative compression of H⋯Cl contacts are consistent with the much weaker volume compression of phase II than that of phase I (cf. Fig. 4 and 5).

The shortest intermolecular contacts in the PCE polymorphs can be represented as the diagram of differences between interatomic distances and the sums of van der Waals radii (Fig. 6).[5] It shows that the shortest contacts (related to the van der Waals radii) are the Cl⋯Cl halogen bonds and only one CH⋯Cl contact in phase I can be compressed to the third shortest value (the third order), before the crystal transforms to phase II. In phase II, the role of CH⋯Cl contacts is considerably reduced to the sixth order. Fig. 6 also illustrates the significantly changing role of contacts CH⋯Cl within phase I. However, the types of shortest contacts in the crystal remain unchanged within the phases and at the phase transition.

Conclusions

In most haloalkanes investigated so far, high pressure favored the CH⋯halogen bonds more than the halogen⋯halogen contacts; however in the high-pressure phase II of C_2HCl_5 the role of the shortest CH⋯Cl bonds is gradually diminished. It can be assumed that the mechanism leading to this type of transformations involves the limited access to the CH site. The H-bonds have been secluded by the requirement of close packing of the bulky molecules, pushing the CH⋯Cl bonded groups apart. This effect illustrates one of
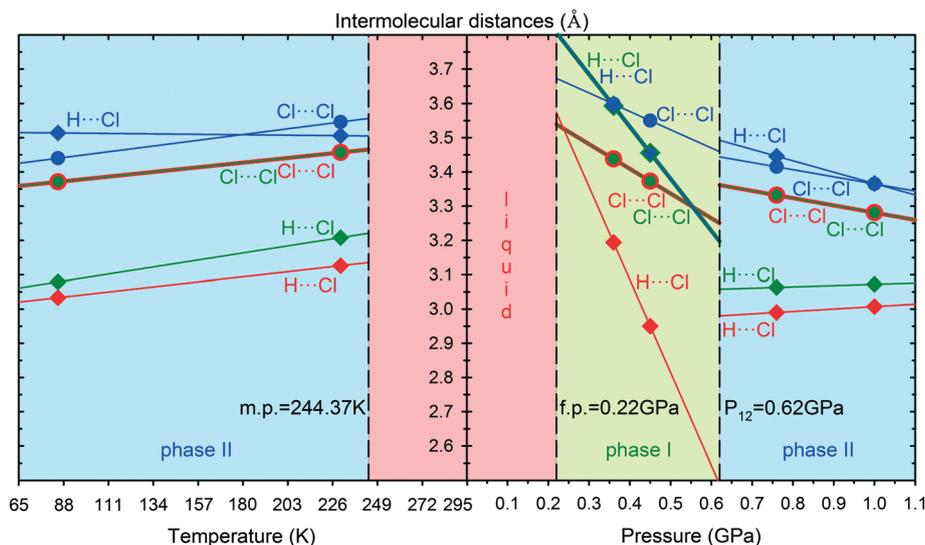

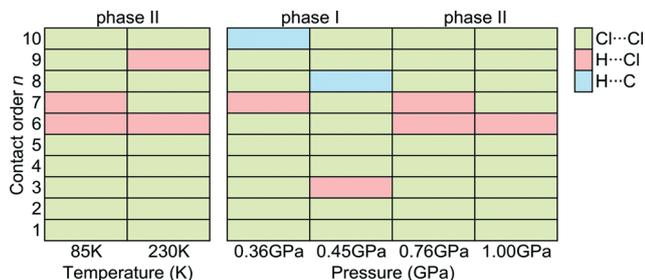**Fig. 5** The shortest H⋯Cl and Cl⋯Cl intermolecular distances (Å) in phases I and II of PCE.

Fig. 6 The contact types arranged into a table according to the increasing values (contacts orders) of smallest contact parameters δ, equal to intermolecular distance minus the van der Waals radii, for PCE phases I and II.

possible mechanisms leading to structural transformations, and in an analogous way to the structures with potential OH···O bond donors and acceptors, but without the OH···O bonds due to steric hindrances.[9] The room-temperature transition at 0.62 GPa in PCE is one of still rare examples of the structures, where the shortest intermolecular contact in the low-pressure phase (I) is shorter than the shortest contact in the high-pressure phase (II). A similar relation was observed between the shortest OH···O bonds in the low- and high-pressure phases of sucrose.[10] Although phases I and II are structurally related, as indicated by the solid–solid transition, unit-cell dimensions, group–subgroup symmetry relation and similar molecular positions, the transformation induces exceptionally strong strain and rearrangement of molecules, which is consistent with the changes in cohesion forces.

Acknowledgements

Notes and references

1   (a) D. Seyferth, *Organometallics*, 2003, **22**, 5154–5178; (b) A. Olejniczak, A. Katrusiak and A. Vij, *CrystEngComm*, 2009, **11**, 1073–1080.

2   M. Podsiadło, A. Olejniczak and A. Katrusiak, *CrystEngComm*, 2014, **16**, 8279–8285.

3   (a) J.-S. Chen, R. B. Shirts and W.-C. Lin, *J. Phys. Chem.*, 1986, **90**, 4970–4975; (b) M. Bujak, M. Podsiadło and A. Katrusiak, *Chem. Commun.*, 2008, 4439–4441.

4   (a) M. Bujak and A. Katrusiak, *CrystEngComm*, 2010, **12**, 1263–1268; (b) M. Bujak, M. Podsiadło and A. Katrusiak, *CrystEngComm*, 2011, **13**, 396–398; (c) M. Bujak, D. Bläser, A. Katrusiak and R. Boese, *Chem. Commun.*, 2011, **47**, 8769–8771; (d) M. Podsiadło, M. Bujak and A. Katrusiak, *CrystEngComm*, 2012, **14**, 4496–4500; (e) Ph. Negrier, M. Barrio, J. Ll. Tamarit, D. Mondieig, M. J. Zuriaga and S. C. Perez, *Cryst. Growth Des.*, 2013, **13**, 2143–2148.

5   M. Kaźmierczak and A. Katrusiak, *CrystEngComm*, 2015, **17**, 9423–9430.

6   (a) F. P. A. Fabbiani and C. R. Pulham, *Chem. Soc. Rev.*, 2006, **35**, 932–942; (b) E. V. Boldyreva, *Acta Crystallogr., Sect. A: Found. Crystallogr.*, 2008, **64**, 218–231; (c) J. Chen, H. Couvy, H. Liu, V. Drozd, L. L. Daemen, Y. Zhao and C.-C. Kao, *Int. J. Hydrogen Energy*, 2010, **35**, 11064–11070; (d) J. Zhao, H. Liu, L. Ehm, D. Dong, Z. Chen, Q. Liu, W. Hu, N. Wang and C. Jin, *Inorg. Chem.*, 2013, **52**, 8067–8073; (e) J. Ridout and M. R. Probert, *Cryst. Growth Des.*, 2013, **13**, 1943–1948; (f) E. V. Boldyreva, *Z. Kristallogr.*, 2014, **229**, 236–245; (g) S. Bergantin, M. Moret, G. Buth and F. P. A. Fabbiani, *J. Phys. Chem. C*, 2014, **118**, 13476–13483; (h) J. Ridout, L. S. Price, J. A. K. Howard and M. R. Probert, *Cryst. Growth Des.*, 2014, **14**, 3384–3391; (i) K. Wang, J. Liu, K. Yang, B. Liu and B. Zou, *J. Phys. Chem. C*, 2014, **118**, 8122–8127; (j) X. Tan, K. Wang, T. Yan, X. Li, J. Liu, K. Yang, B. Liu, G. Zou and B. Zou, *J. Phys. Chem. C*, 2015, **119**, 10178–10188.

7   (a) A. Bondi, *J. Phys. Chem.*, 1964, **68**, 441–451; (b) S. C. Nyburg and C. H. Faerman, *Acta Crystallogr., Sect. B: Struct. Sci.*, 1985, **41**, 274–279; (c) S. S. Batsanov, *Inorg. Mater.*, 2001, **37**, 871–885.

8   (a) G. R. Desiraju and R. Parthasarathy, *J. Am. Chem. Soc.*, 1989, **111**, 8725–8726; (b) V. R. Pedireddi, D. S. Reddy, B. S. Goud, D. C. Craig, A. D. Rae and G. R. Desiraju, *J. Chem. Soc., Perkin Trans. 2*, 1994, 2353–2360; (c) L. Brammer, E. A. Bruton and P. Sherwood, *Cryst. Growth Des.*, 2001, **1**, 277–290; (d) M. Fourmigué, *Curr. Opin. Solid State Mater. Sci.*, 2009, **13**, 36–45; (e) F. F. Awwadi, R. D. Willett, K. A. Peterson and B. Twamley, *Chem. – Eur. J.*, 2006, **12**, 8952–8960; (f) A. Mukherjee, S. Tothadi and G. R. Desiraju, *Acc. Chem. Res.*, 2014, **47**, 2514–2524.

9   (a) C. P. Brock and L. L. Duncan, *Chem. Matter.*, 1994, **6**, 1307–1312; (b) C. P. Brock, *Acta Crystallogr., Sect. B: Struct. Sci.*, 2002, **58**, 1025–1031.

10 E. Patyk, J. Skumiel, M. Podsiadło and A. Katrusiak, *Angew. Chem., Int. Ed.*, 2012, **51**, 2146–2150.